INTERFACE

rsif.royalsocietypublishing.org

Research

Cite this article: Rieu J-P, Delanoë-Ayari H, Takagi S, Tanaka Y, Nakagaki T. 2015 Periodic traction in migrating large amoeba of *Physarum polycephalum*. *J. R. Soc. Interface* **12**: 20150099.
http://dx.doi.org/10.1098/rsif.2015.0099

Received: 6 February 2015
Accepted: 26 February 2015

Subject Areas:
biophysics, biomechanics

Keywords:
amoeboid motility, traction force microscopy, physarum, actomyosin contractility, birefringence

Authors for correspondence:
Jean-Paul Rieu
e-mail: jean-paul.rieu@univ-lyon1.fr
Toshiyuki Nakagaki
e-mail: nakagaki@es.hokudai.ac.jp

Electronic supplementary material is available at http://dx.doi.org/10.1098/rsif.2015.0099 or via http://rsif.royalsocietypublishing.org.

THE ROYAL SOCIETY PUBLISHING

Periodic traction in migrating large amoeba of *Physarum polycephalum*

Jean-Paul Rieu[1], Hélène Delanoë-Ayari[1], Seiji Takagi[2], Yoshimi Tanaka[3] and Toshiyuki Nakagaki[2,4]

[1]Institut Lumière Matière, UMR5306 Université Lyon 1-CNRS, Université de Lyon, 69622 Villeurbanne cedex, France
[2]Research Institute for Electronic Science, Hokkaido University, N20W10, Sapporo 060-0806, Japan
[3]Graduate School of Environment and Information Sciences, Yokohama National University, 79-7 Tokiwadai, Hodogaya-ku, Yokohama 240-8501, Japan
[4]JST, CREST, 5, Sanbancho, Chiyoda-ku, Tokyo 102-0075, Japan

The slime mould *Physarum polycephalum* is a giant multinucleated cell exhibiting well-known Ca^{2+}-dependent actomyosin contractions of its vein network driving the so-called cytoplasmic shuttle streaming. Its actomyosin network forms both a filamentous cortical layer and large fibrils. In order to understand the role of each structure in the locomotory activity, we performed birefringence observations and traction force microscopy on excised fragments of *Physarum*. After several hours, these microplasmodia adopt three main morphologies: flat motile amoeba, chain types with round contractile heads connected by tubes and motile hybrid types. Each type exhibits oscillations with a period of about 1.5 min of cell area, traction forces and fibril activity (retardance) when fibrils are present. The amoeboid types show only peripheral forces while the chain types present a never-reported force pattern with contractile rings far from the cell boundary under the spherical heads. Forces are mostly transmitted where the actomyosin cortical layer anchors to the substratum, but fibrils maintain highly invaginated structures and contribute to forces by increasing the length of the anchorage line. Microplasmodia are motile only when there is an asymmetry in the shape and/or the force distribution.

1. Introduction

The plasmodium *Physarum polycephalum*, a true slime mould, has been used as a model organism in studies analysing cell movement [1]. The plasmodium is a giant single cell with multiple nuclei and is composed of a highly invaginated outer layer of gel protoplasm (the ectoplasm) and a sol-like inner protoplasm (the endoplasm). The sol-like protoplasm exhibits streaming movements caused by the periodic contraction of large actomyosin fibrils in the ectoplasm [2]. Contraction occurs when the fibrils are formed, and it ends when the fibrils dissociate [3]. It has been shown previously that formation and dissociation can be measured by birefringence measurements and are associated with area changes [4]. Because major components of the periodic contraction mechanism are F-actin and myosin, intracellular Ca^{2+} has been suggested to play an important role in control of the movement: an elevation in $[Ca^{2+}]$ induces cell contraction [5].

The direction of streaming reverses at regular intervals (shuttle streaming) owing to differences in internal pressure which reverses in response to the cycle of contraction–relaxation movements and in response to complicated spatial phasing [6,7]. Fragments of plasmodia (microplasmodia) may exhibit regular shuttle streaming, move and change shape actively depending on their shapes. A variety of shapes have been examined, including a thinly spread plasmodium of amoeboid type, spherical types or chain types where spherical contractile heads are connected by tubular parts like a dumbbell shape with two spheres and a single connecting tube (figure 1*a*,*b*). In spite of

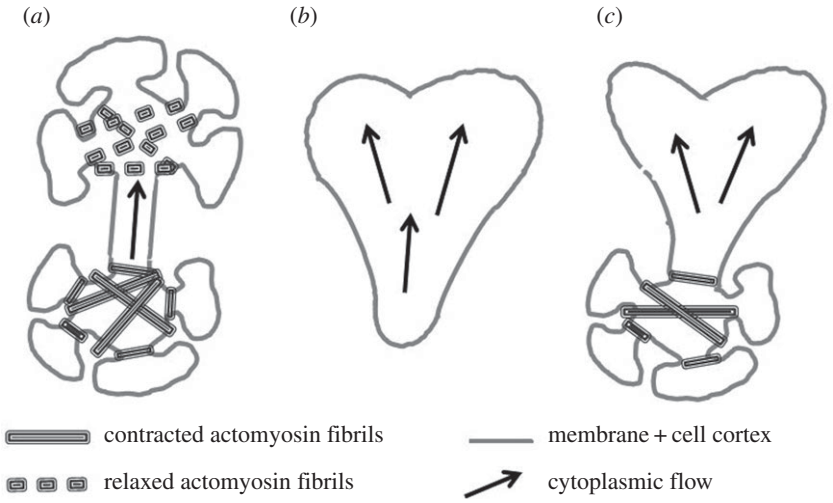

Figure 1. Schematic drawing of the three main types of microplasmodia. The interface of each cell type consists of a cell membrane and an underlying thin actomyosin cortical layer. This layer is contractile and both its thickness and its effective tension may vary in space and time. (*a*) The chain type consists of several highly invaginated spherical heads connected by tube parts; these heads are highly contractile in particular due to the presence of large actomyosin fibrils which assemble (bottom head) and disassemble (top head) periodically. (*b*) Amoeboid type characterized by a flat shape, highly irregular and only a cell cortex. (*c*) Hybrid type characterized by a combination of the other two types. In each type, cytoplasmic flows (large arrows) are generated by the contractile activity of cell cortex and fibrils (adapted from Gawlitta *et al*. [8]).

the marked variability in cell shape causing internal cytoplasmic flow (arrows in figure 1), amoeboid type shows only little locomotory activity as compared with similar irregularly shaped *Amoeba proteus* [9]. Neither invaginations nor contractile fibrils are encountered in this type; however its cortex is surrounded by a thin actomyosin cortical layer [8]. Chain type microplasmodia possess both an actomyosin thin cortical layer everywhere around the peripheral as well as periodically contracting fibrils and invaginations in the spherical heads. One can define a third type of microplasmodium that we call here the hybrid type (figure 1*c*) asymmetric in shape and constituted of areas both with and without contractile fibrils and invaginations.

In order to move on surfaces, living organisms need to exert forces on their substrate. So far, traction force measurements have been mostly performed on slow cells strongly adhering to their substrate, but very few studies have been performed on larger or multicellular organisms [10,11]. In the case of *Physarum*, there exists a characteristic variety in cell shapes that correlates with locomotion activity, periodic contractions and large-scale cytoplasmic flows as described above. In order to build a global model of amoeboid locomotion, it is essential to measure as well the traction force patterns generated during locomotion for each cell type.

2. Material and methods

2.1. Preparation of plasmodia for traction force microscopy and birefringent observations

All cultures and experiments were conducted at 25°C. Plasmodia of *P. polycephalum* were grown on oat flakes for 2 days in troughs ($35 \times 25\ \mathrm{cm}^2$) under dim light. Tiny portions were cut from the front tips of the plasmodia and placed on a plain agar plate (1.5%, 9 cm diameter). After waiting overnight until the plasmodial pieces were moving and had tubular shapes, portions of their tips were again removed. For traction force microscopy experiments, they were placed on collagen-coated polyacrylamide gels for several hours before observation.

For birefringent observations, a thin-spread small plasmodium (approx. 30 µm in thickness) was prepared according to the method previously reported [4]. A small portion of protoplasm ($0.2 \times 0.2\ \mathrm{mm}^2$) was cut out from a larger plasmodium ($1 \times 2\ \mathrm{mm}^2$) under a binocular microscope (Nikon SMZ1500) and the cut portion was placed on a plain agar plate and was overlaid with a coverslip. After half a day, it extended and moved on the agar and served for the observation of birefringent fibres.

2.2. Polyacrylamide gels

Flexible polyacrylamide gels for traction force microscopy were prepared with slight modifications from standard protocols [10]. Typical composition was the following: 10% acrylamide solution (Bio-Rad), 0.03% bis solution (Bio-Rad), 10% v/v of a 2% solid 1 µm fluorescent bead solution (Red F-8821, Molecular Probes). After degassing for 30 min, 1/100 v/v and 1/1000 v/v of a 10% w/v ammonium persulfate solution and TEMED, respectively (both Bio-Rad products) were added and two separate 170 µl droplets of the mixture were deposited on an untreated hydrophobic 24×60 mm cover glass (Matsunami, Japan). A 25 mm circular hydrophilic untreated cover glass (Fisher brand) was deposited on the droplets. After polymerization (15–30 min), the hydrophilic glass was removed under water, and the gel was covalently coated with type I collagen (Wako Chemicals, Japan) using Sulfo-SANPAH (Pierce Chemical, Rockford, IL, USA) in order to allow cell adhesion. Young's modulus E and the thickness of the gel were measured as 6.0 ± 0.4 kPa and 400 µm, respectively. The Poisson ratio v of polyacrylamide gels was taken as 0.5 [10].

2.3. Traction force microscopy

Traction force microscopy is based on the observation of substratum deformation (here, thanks to fluorescent beads embedded inside the gel) and subsequent force calculations. Deformations were measured with a confocal microscope (Olympus IX70-KrAr-SPI) using 10× or 20× objectives. We simultaneously visualized the cell contours (transmission channel) and the bead positions (fluorescence channel, 568 nm line). Images were recorded and analysed during a period of about 15 min at an interval of $\delta t \sim 10$ s. The focus plane z_B was fixed carefully at about -10 µm from the gel/cell surface. Bead displacements

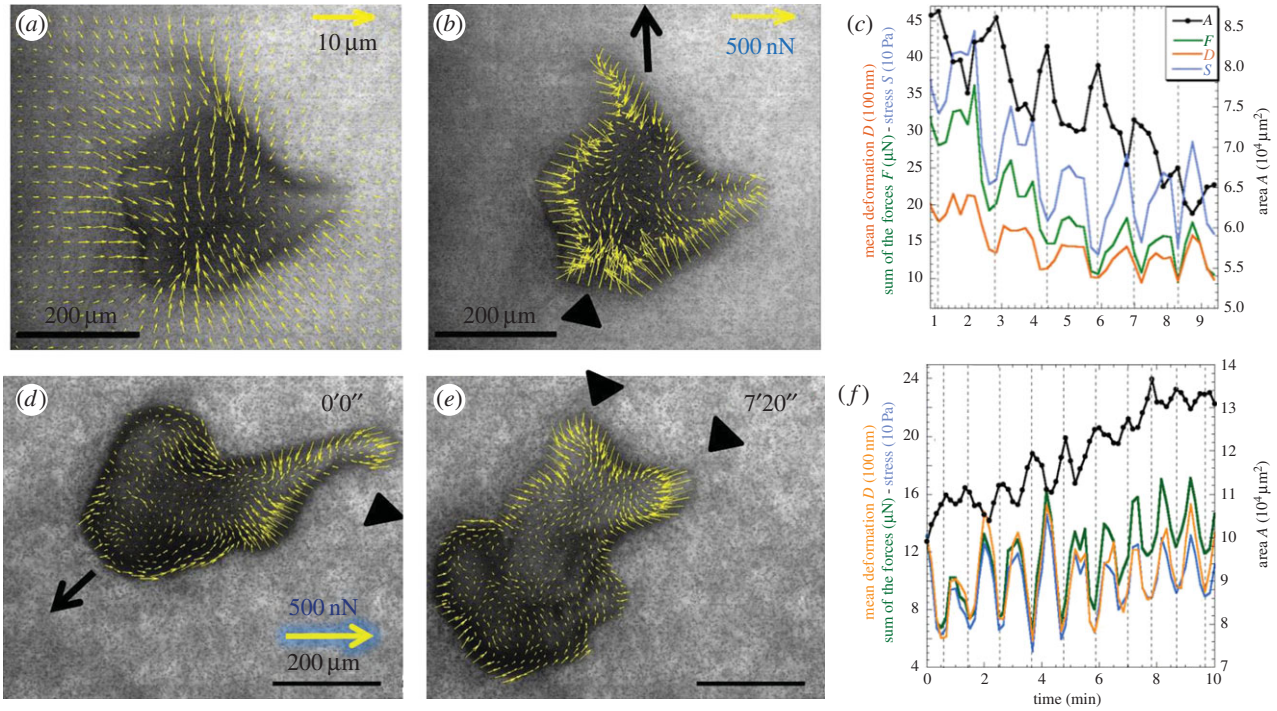

Figure 2. Deformation and force field of two amoeboid type microplasmodia. (*a*) PIV deformation field and (*b*) corresponding force field of a first amoeboid microplasmodium slowly moving towards the top (arrow in *b*). (*d*,*e*) Force field at 0 and 7 min 20 s of another amoeboid microplasmodium moving quickly towards bottom left (arrow in *d*) and experiencing large shape changes. Forces are very peripheral almost absent from the inner region, always directed centripetally (inwardly) and maximum in the rear parts (arrowheads). (*c*,*f*) For each microplasmodium, the sum of the forces F (in micronewtons, green line), the mean bead deformation D (in units of 100 nm, orange line) and the stress S (in units of 10 Pa, blue line) oscillate in phase opposition with the oscillations of area A (in units of 10^4 µm^2, black line). Vertical dotted lines corresponding to peaks of cell area (i.e. maxima). The mean interval between lines (i.e. period of contraction–relaxation cycles) is $T = 1.6$ min in (*c*), $T = 1$ min in (*f*).

D_i were calculated by particle image velocimetry (PIV) from a reference frame which was recorded at the end of the experiment once the microplasmodium was detached from the substratum by gently pipetting the medium around it. We used the toolbox mPIV (http://www.oceanwave.jp/softwares/mpiv/) written for Matlab (http://www.mathworks.com). A recursive algorithm beginning with a window size of (64 × 64) pixels, ending with a window size of (16 × 16) pixels, and a 50% overlap between windows was typically set. We inverted the Fredholm integral equation relating substrate deformations to traction forces using the package of Matlab routines Regularization Tools by P. C. Hansen (http://www.netlib.org/) already adapted for *Dictyostelium* single cells and slugs [10,12]. The L-curve of zero-order Thikonov algorithm is used to calculate the value of the regularization parameter, and we approximate the force pattern by an ensemble of localized point-like forces F_i under a triangular mesh generated under the cell by a Delaunay triangulation (Matlab pde toolbox). We compute the overall force as F and stress S as $F = \Sigma\|F_i\|$ and $S = F/A$, where F_i is the force under a given triangular mesh unit cell and A is the cell area. We also compute the mean deformation D under the cell as $D = \text{mean}(D_j)$, where D_j is the deformation under a given PIV mesh unit cell j and the mean is performed under unit cells under the cell only.

2.4. Birefringent microscopy

The organism was observed by an advanced polarized light microscope, an LC-Pol Scope. This microscope can detect birefringence in all directions in two-dimensional plane by combining liquid-crystal devices with the polarizer [13]. In this system, the liquid-crystal device with the polarizer is placed before the condenser in the illumination optical path of the upright microscope (Nikon Eclipse 80i) and the analyser is placed after the objective lens. Birefringence was observed by monochromatic light of $\lambda = 546$ nm using 40× objectives at intervals of 2 s. In the observed birefringent images, the parts with a higher retardance, i.e. a larger phase shift between the fast and slow axes of birefringence, are indicated by brighter level of black-and-white grey scale, the brightest indicating 6 nm shift and the darkest indicating no phase shift. According to previous studies [4,14], the high birefringence came from thick bundle of filamentous actin, or intermediate filaments. The birefringent fibril structures were observed most sharply and clearly at the dorsal layer of the plasmodium.

3. Results

Microplasmodia of *P. polycephalum* (300–800 µm long) are able to exert regular rhythmic activity and streaming, and they are able to migrate on collagen-coated soft polyacrylamide. They induce large displacements of fluorescent beads (i.e. about 5 µm at $z_B = -15$ µm) when using a substratum of Young's modulus $E = 6$ kPa (figure 2*a*; electronic supplementary material, movie M1). For larger microplasmodia, we sometimes observed deformations far from the cell body that we interpreted as the contractile effect of secreted slime adhering on the substrate. We selected only microplasmodia for which deformations were vanishing at long distances. Forces were calculated using explicit regularization techniques already developed for *Dictyostelium* single cells [12] and slugs [10,11]. They are always directed centripetally whatever their type (figures 2–6). The total force (sum of absolute values of forces under the organism) lies in the range 10–30 nN. We now present traction force measurements for the three typical microplasmodia types:

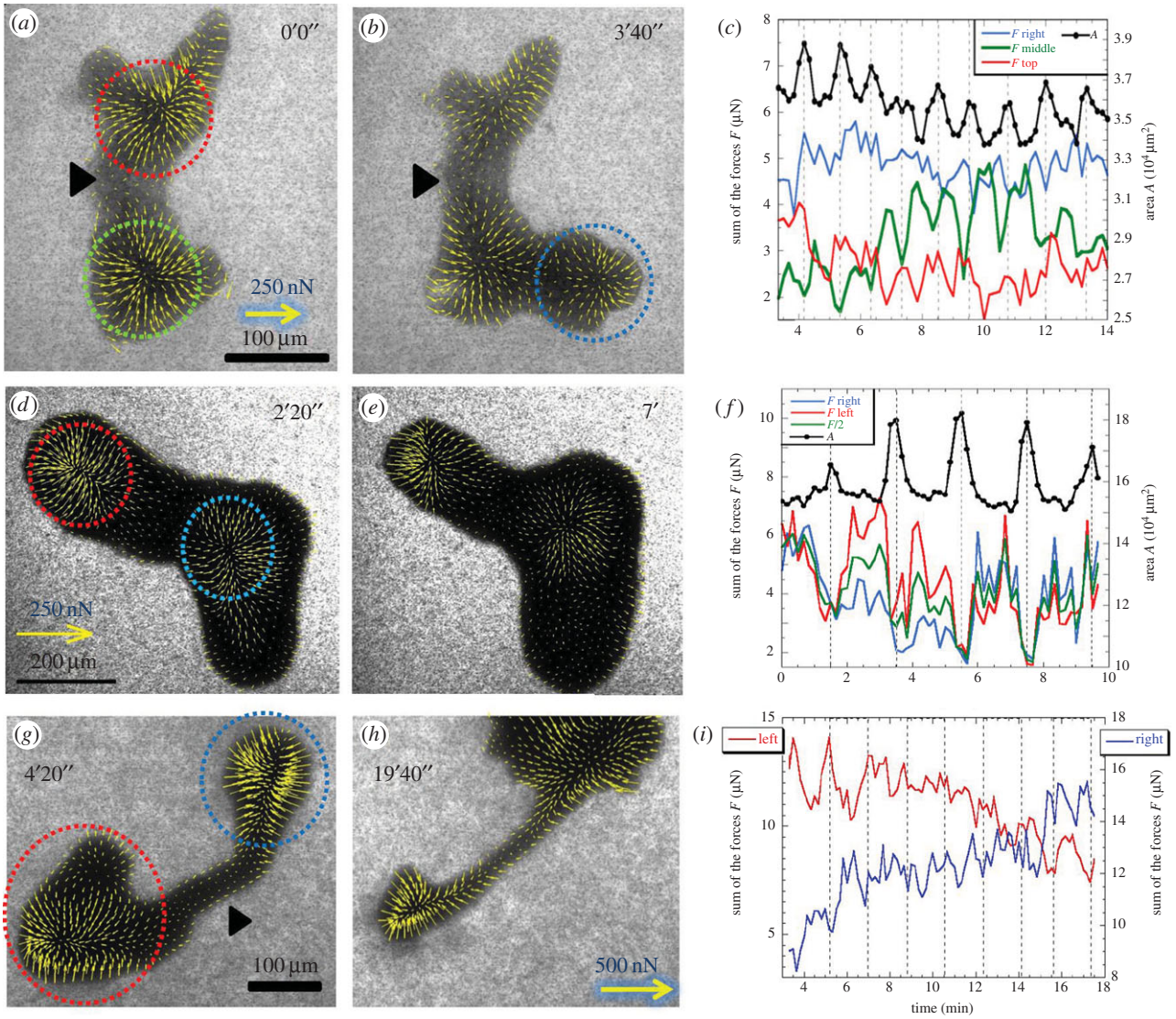

Figure 3. Force field of three chain type microplasmodia. (*a*) Initially, the first one presents two main circular contraction units (surrounded by dotted circles) where force vectors converge centripetally. (*b*) Later, it expands a pseudopod on the right and a new centripetal contraction unit is created (blue circle). (*c*) Time series of cell area and force changes in zones surrounded by dotted circles in (*a*,*b*). The middle zone (green circle) exhibits force oscillations in phase opposition with area. The interval between peaks of area (vertical dotted lines) is $T = 1.15$ min. (*d*–*f*) The second microplasmodium, not moving, has two synchronized contractile units in phase opposition with area oscillations ($T = 2.1$ min). (*g*) The third one has a dumbbell shape. Forces are not transmitted to substratum under the long central connecting tube (arrowhead). (*h*) Later, the bottom-left contractile unit progressively shrinks and the other one grows. (*i*) Forces in the two contractions units mostly oscillate in counter-phase.

(1) amoeboid types with irregular and changing shape which appear rather flat as deduced from the lighter contrast detected by the transmission channel of the confocal microscope (figure 2);
(2) chain types formed of thick rounded heads connected by tube strands. They are either dumbbell-shaped connected by a long cylindrical tube (figure 3*g*–*i*) or with several juxtaposed heads with little tube portion in between: two heads as in figure 3*d*–*f* or three heads as in figure 3*a*–*c*; and
(3) hybrid types (figures 6 and 7).

There is a clear difference in terms of force distribution between the first two types but note that a given microplasmodium may change its type in the course of time (figure 5). Amoeboid microplasmodia exert mostly peripheral force with little force in the inner part of the cell/substratum contact area (figure 2*b*,*d*,*e*). When they are motile, they generally take a polarized shape with strong retracting forces in the narrower tails (figure 2*d*,*e*; electronic supplementary material, movie M2). The more striking feature of these measurements is the fact that substrate deformations, forces or stress are oscillating with an impressive regularity ($T = 1$–2 min, figure 2*c*,*f*) and that this oscillation is in counter-phase with the well-known rhythmic change of cell area. When the cell contracts (minimum cell area), forces increase and when the cell relaxes (area is maximum) forces decrease.

Chain types exert still inwardly oriented forces on their substratum but more internally distributed all around a contractile unit centred under the rounded heads (surrounded by dotted lines in figure 3*a*,*b*,*d*). The dumbbell shape type is constituted of two contractile units separated by a long tube (figure 3*g*). The tube part of the dumbbell-shaped microplasmodia does not transmit significant forces to the substratum (see arrowhead in figure 3*g*). This is also the case for other more compact chain types (see for instance in figure 3*a*,*b* the near absence of forces in the region

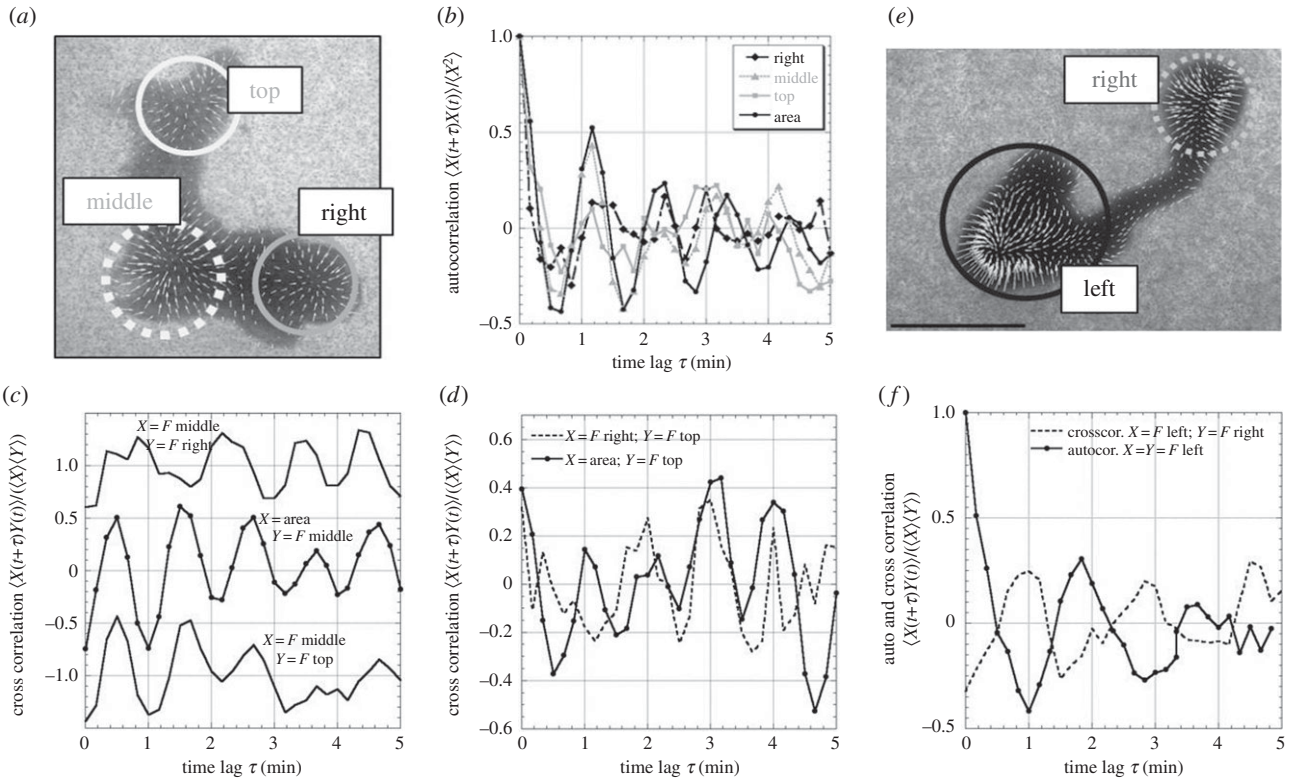

Figure 4. Auto and cross correlations of contraction units. (*a*) The chain type microplasmodium with three contraction units of figure 3*a*–*c* exhibits regular oscillations of each contraction unit as well as cell area (*b*). The middle contraction unit is in counter-phase with the top and right contraction units as well as with the area (*c*). Top and right contraction units as well as area are in phase (*d*). (*e*,*f*) The two separated contraction units of dumbbell-shaped microplasmodia oscillate in counter-phase. For (*c*) the top and bottom curves have been shifted by +1 and −1, respectively, to avoid overlapping.

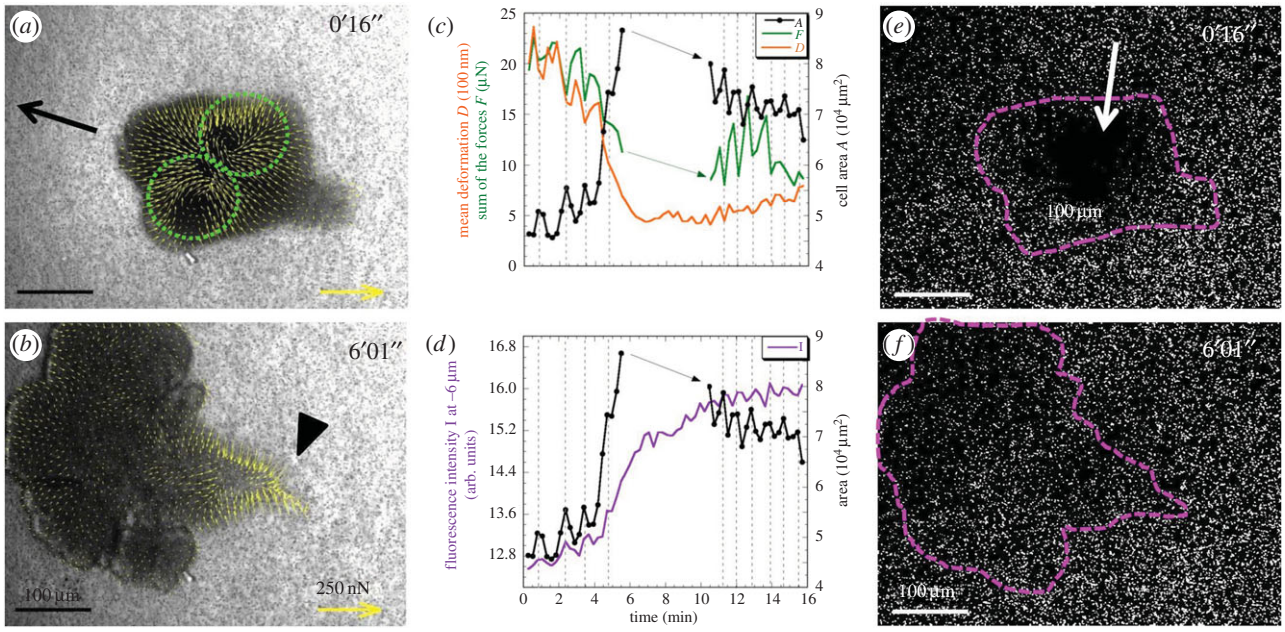

Figure 5. Transition from thick chain type to a hybrid type. An initially small and thick microplasmodium with two juxtaposed contraction units (dotted circles in *a*) suddenly spreads and moves towards the left (*b*). Forces in this hybrid type microplasmodium are near the periphery but weaker in the front pseudopod than in the retracting tail (arrowhead in *b*) and absent in the bottom part. (*c*) The transition towards the hybrid type is evidenced by an area *A* increase (black line with dots) and simultaneously by a decrease in the mean bead deformation *D* (orange line) and overall force *F* (green line). Missing points in (*c*,*d*) are due to the fact that a part of the microplasmodium is outside the field of view. (*e*,*f*) Fluorescence images measured at $z_B = -6$ µm from the gel/cell contact plane, showing a clear depletion of fluorescent beads exactly where the contraction unit is located when the cell is thick and globular (arrow in *e*) but little vertical deformation when the cell is hybrid (*f*). (*d*) The fluorescence intensity I (purple line) under the cell as a function of time indicates the amount of beads out of focus.

indicated by arrowheads in between the two contractile units). These chain type microplasmodia are also periodically expanding and contracting their overall area and their contractile units exert periodic forces as well but not always with a simple counter-phasing with cell area (figure 3*c*,*f*,*i*). The first investigated microplasmodium, from a two-head configuration (figure 3*a*) quickly expands a third contracting head (figure 3*b*; electronic supplementary material, movie

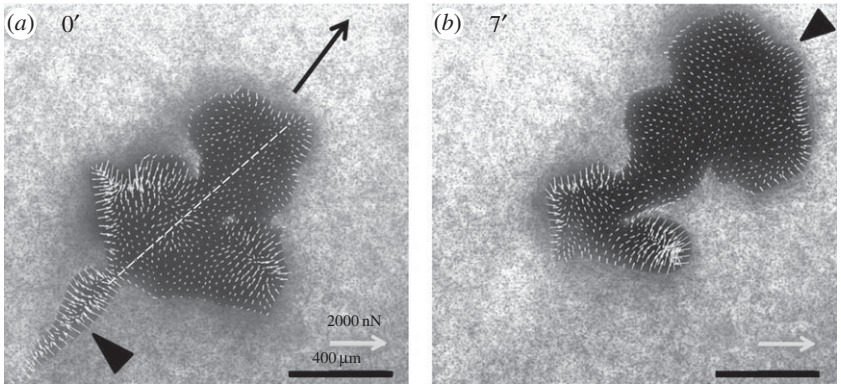

Figure 6. Force field of a large motile hybrid microplasmodium. The giant cell migrates fast (51 µm min^{-1}) towards the top right of the image at two different times. The force map presents initially a very narrow retracting tail (*a*) with strong retraction forces mostly perpendicular to the long tail axis (arrowhead). This tail disappeared 7 min later (*b*). Two posterior contractile units on the side symmetric to the anterior–posterior axis (dotted line in *a*) exert large contracting forces directed centripetally (*b*). These regions slowly shrink with time as the front expands (*b*). In the front, forces are small except at the very periphery where they are inwardly directed (arrowhead in *b*).

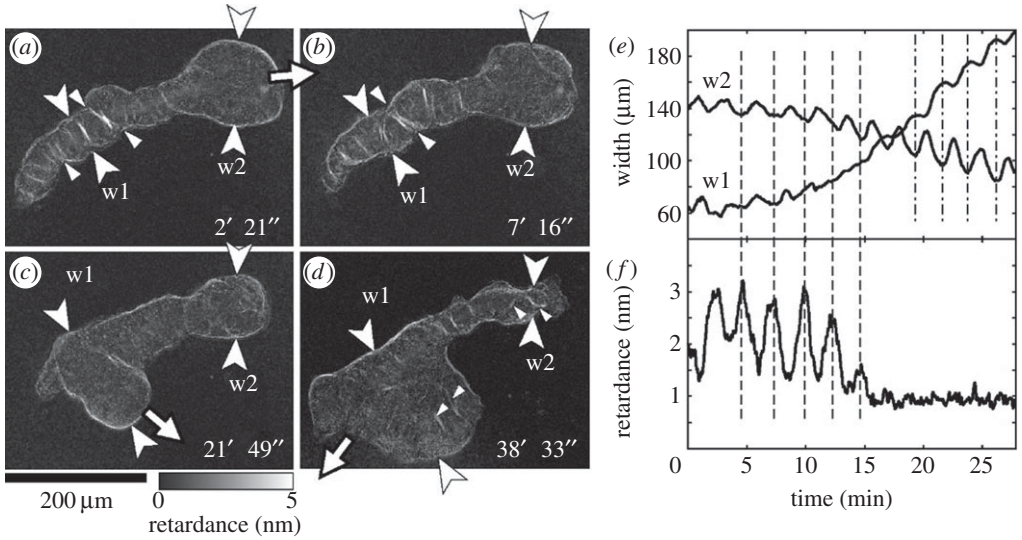

Figure 7. Birefringence imaging of moving microplasmodium. (*a–d*) Retardance images at four different times. (*e*) Time series of width of body measured at two different parts of w1 and w2. (*f*) Time course of retardance of thick fibrils at a part where the width w1 was measured. Vertical broken lines in (*e*,*f*) correspond to the times of maximum retardance. Vertical dashed-dotted lines in (*e*) correspond to minimum of w2.

M3). The rhythmic changes of forces (in each contracting unit) and of area exhibit the very same period ($T = 1.15$ min; figure 4*b*). The top and right contraction units are oscillating in phase with each other and with the area changes (figure 4*c*). The middle unit on the other hand is in phase opposition with area changes and other contraction units (figure 4*d*). The second chain type microplasmodium investigated presents two heads perfectly oscillating in phase with each other and in counter-phase with the area (figure 3*d–f*; $T = 2.1$ min). In the case of the dumbbell shape (figure 3*g–i*; electronic supplementary material, movie M4), the contractile forces exerted by the two heads are almost in perfect counter-phase (figure 4*e*,*f*). At the end of the series, the bottom-left head progressively shrinks and retracts and the top-right grows generating a net displacement.

Figure 5 presents an example of a phenotypic transition. Initially, this chain type microplasmodium presents two juxtaposed contractile units (dotted circles in figure 5*a*). After some time, it suddenly spreads and changes to a motile hybrid type with forces concentrated in the retracting tail and in the front periphery (figure 5*b*). Cell area increases threefold while force drops twofold around $t = 4.5$ min (figure 5*c*). Another important difference between hybrid and chain types is the vertical component of forces transmitted to the substrate. We can appreciate it from the examination of bead defocusing under the cell (figure 5*d–f*). Before the transition, fluorescent images of beads show a black hole under the contractile rounded head at a depth of $z_B = -6$ µm from the estimated elastic substratum/medium interface (arrow in figure 5*e*) indicating that surface beads are pushed downward by more than this distance. Vertical deformations are therefore of the same order or larger than in-plane ones. After the transition, beads are well focused under the hybrid type microplasmodium (figure 5*f*; see also the electronic supplementary material, movie M5). We have computed the mean grey value under the cell (figure 5*d*). A low grey value (i.e. strong defocusing or absence of beads) indicates that the cell exerts downward oriented pushing forces, a high grey value (i.e. many bright beads in the field) indicates low normal forces. This quantity oscillates before and after the transition with the same period as other signals (area, deformations, forces, etc.); beads are more defocused when the cell is contracting. Interestingly, the period of rhythmic oscillations is lower in the hybrid type

than in the chain type ($T = 1$ and 1.33 min, respectively), the sum of the forces being almost half as great in hybrid type (figure 5*c*). Further investigations over longer times would be necessary to investigate more precisely these transitions.

The last presented experiments complete the small panel of microplasmodia shapes. It corresponds to a big hybrid type, multiheaded in the posterior region, more amoeboid in the anterior region, very motile, roughly symmetric with respect to the anterior–posterior axis (dotted line in figure 6*a*). Along this axis, large retraction forces are encountered in the retracting tail (arrowhead) until this tail disappears (figure 6*b*). Interestingly, these forces are not parallel to this anterior–posterior axis but really perpendicular to it. Right after the tail in the posterior region, two opposite contraction units are present with centripetal forces. In the quickly expanding front region, forces are absent except at the very front part where they are oriented inwardly.

We have performed birefringent observations in order to establish a correspondence between the traction forces and the presence of contractile fibres in particular for the hybrid type microplasmodia that were not classified in previous studies. Figure 7 shows the birefringent image of such a moving hybrid type microplasmodium with a body shaped like a tadpole (see also the electronic supplementary material, movie M6). In the tail part (w1 in figure 7*a*,*b*), thick and long bundles of filaments extended throughout the full width of the tail. This means that the fibres bound the width of the tail when contracting. Mechanical tension produced by active contraction acted not only between local part but also over global distance of the whole organism. Such thick and long bundles of filaments as observed in the tail were not observed in the frontal amoeboid type region (around w2 in figure 7*a*,*b*). In the posterior half of the microplasmodium, concave parts of body shape were often observed (indicated by the small arrowheads in figure 7*a*,*b*) and the filaments attached to these concave parts. So the presence of large fibres was closely related to formation and maintenance of the concave shape of the cell body.

Between 2 and 6 min in figure 7*e*, the left tail (w1) and the head (w2) contracted simultaneously, and the peak of retardance of the filaments at the tail corresponded to the peak of contraction (minima of the body width) as indicated by the broken lines in figure 7*e*,*f*. This correspondence continued up to 7 min. The thick bundles of filaments were formed at an interval of 10–50 µm along the tubular tail and tied up the tail in the direction perpendicular to the long axis of the plasmodium. Although the plasmodium had migrated towards the top right before 2 min (indicated by the arrow in figure 7*a*), it almost stopped migrating between 2 and 6 min in figure 7*e*.

After 7 min, the widths at w1 and w2 started to increase and decrease, respectively, while the contraction rhythms between w1 and w2 switched from in-phase to out-of-phase (see figure 7*e* in the time 15–25 min). The plasmodium started to migrate in a different direction from the previous one as indicated by the arrow in figure 7*c*. Then the thick bundles at the tail disappeared; the retardance of the bundles at w1 decreased to a low level and the oscillation of the retardance was also lost (figure 7*f*). After 38 min, thick bundles were formed around w2 and also at some distance from the periphery around w1 (the small arrowheads in figure 7*d*); this plasmodium started to move in the other direction as indicated by the arrow in figure 7*d*.

4. Discussion

Protoplasmic streaming activity and locomotion in plasmodia of *P. polycephalum* are intimately correlated with the fine structure of the organism at the micrometre and nanometre scales, in particular with the presence of actomyosin large fibrils and invaginations [1]. Small fragments of plasmodium called microplasmodia are especially suited to elucidate the relationship between structure and dynamics in amoeboid cells. While there is no doubt that actomyosin structures participate to the motive force [1,2,7,8,14–16] no direct measurements of the force exerted on their substrate have been made to date. This work presents the first traction force maps of the main types of microplasmodia and the first discussion of them in relation to their structure.

(1) Amoeboid types are very irregular with small membrane indentations. They are essentially free of large membrane invaginations such as those found for veins of large plasmodia [17] or chain type microplasmodia [8]. A continuous thin cortical layer (about 0.2 µm thick) consisting of actin and myosin is associated with the plasma membrane (figure 1*b*). The measured force map of amoeboid microplasmodia is similar to that of another amoeboid cell, *Dictyostelium discoideum* [18] with mostly peripheral forces inwardly directed (figure 2). Hence, we can speculate that forces in amoeboid microplasmodia are transmitted to the substratum by the cortical layer at the peripheral contact line with a geometrical contact angle θ with the substratum smaller than 90° (figure 8*b*). But as compared to *Dictyostelium* cells, amoeboid microplasmodia are relatively weakly polarized (i.e. little front–rear asymmetry) in terms of both shape and traction force [8].

(2) Microplasmodia of the chain type are traversed by an extended array of invaginations (often several tenths of a micrometre deep) in the ectoplasmic region of their thick heads. A thin actomyosin cortex is present all around the plasma membrane in the peripheral as well as in the invaginated regions [8]. In addition, the cells possess a contractile fibrillar system anchored at the invaginations (in particular at their basal surface) and running through the cytoplasm. The presence of these actomyosin fibrils is correlated with the well-organized large-scale shuttle streaming [1]. They are abundant in the contractile heads but absent in connecting tubes in between these heads and they are absent in amoeboid types [8]. Here, we show that traction forces of such chain types are transmitted to the substrate mostly under the spherical heads, not under the tube parts (figure 3). This suggests that the tubes are either not contractile (e.g. due to the absence of fibrils) or not tightly anchored to the substratum. Forces are inwardly directed under the spherical heads, the largest force vectors being encountered far from the periphery all around a ring of about $R = 50$ µm radius (figure 3). Such annular contractile units have never been reported in the literature to date.

(3) Hybrid types are asymmetric and motile. They possess areas both with and without contracting fibrils. Although we could not perform simultaneous traction force and birefringence experiments, we show that traction forces are mostly exerted in their posterior part (figure 6)

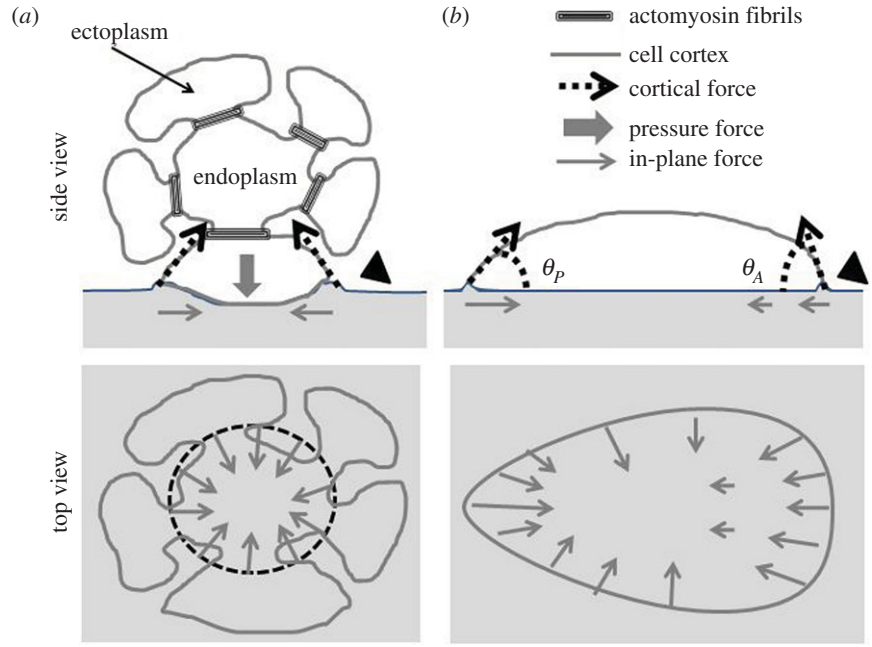

Figure 8. Model of force transmission to the substratum for two kinds of microplasmodia. (*a*) Cross section of the head of a chain type microplasmodium: the invaginated ectoplasm attaches in the inner part of the contact area with a contact angle lower than 90°; cortical forces transmitted to substratum are tangential to the invagination pockets and in-plane component is inwardly directed; an internal pressure inside the pocket counterbalances the forces in the vertical direction; fibrils maintain the pocket shape and possibly enhance cortical tension. (*b*) Cross section of an amoeboid microplasmodium: all forces are exerted by the peripheral cortex and oriented along the cell contact profile defined by the geometrical contact angles θ_P and θ_A. The cortex force is deforming the substrate upward in both cases (arrowheads on the right of (*a*,*b*)) but this deformation was not detected.

where thick bundles of filamentous actin (fibrils) are visible (figure 7). The force, the width and the fibrils (retardance) are periodically contracting.

These observations indicate that both the fibrillar chain types and cortical amoeboid types are exerting periodic forces with a similar period of 1–2 min and a similar range of total force (a few tens of micronewtons for all microplasmodia investigated; figures 2–6). This means that actomyosin contractility is triggered by the same molecular signal (probably calcium level [5]) whatever its fine structure (filamentous cortex or fibrils). For amoeboid microplasmodia, one can estimate the cortical tension transmitted to the substrate by simply dividing the peripheral force by the perimeter L, $\tau_C = F/L = 5$–20 mN m^{-1}, a value intermediate between the ones previously measured for *Dictyostelium* at single cell and slug stages, respectively [11,18]. For chain type microplasmodia, assuming that the force per contractile unit (typically about 5 µN) is mostly transmitted all around a ring of about $R = 50$ µm radius (dotted line in figure 8*a*), we can estimate a head tension $\tau_H = F/2\pi R \simeq 30$ mN m^{-1}, a value quite similar to τ_C. The reason might be that the fibrils themselves do not directly transmit the force to the surface, but they structure the folds and the anchoring points of the cell cortex with the substratum. By increasing the cell/substratum/medium contact line, they increase the total force under the cell (figure 8*a*). It is well known that the invagination system of *Physarum polycephalum* is highly dynamic and enables the plasmodium to adapt its surface to the varying conditions of the environment, and consequently to its own physiological state [15]. The fibrils are assumed to control the closure and opening of invagination which in turn control shuttle streaming [1]. They might also control the internal pressure in the cytoplasm pockets between invaginations which contribute to the downward pushing force detected as a black hole in figure 5*e* and to the cortical tension. In order to check this cortical tension model, it would be interesting in the future to perform high-resolution four-dimensional (*xyzt*) force measurements of the microplasmodia.

These experiments question us on the very early mechanisms for breaking cellular symmetry in cells and organisms. We have found asymmetries in forces, shape and fibrillar distribution along the anterior–posterior axis of moving microplasmodia (figures 2, 5*b*, 6 and 7) but what is the prerequisite to initiate cell motion from a symmetric and non-moving microplasmodium?

Implicitly, most mechanical models of single-cell migration assume a front–rear asymmetry (polarity) in shape and/or cytoskeleton structure to generate net forward motion. Cells may move in two dimensions by retrograde actin flow in the leading lamellipodium and simultaneous actomyosin contraction in their rear or by blebbing (inflated protrusion after the rupture of the front cortex) [19]. A softer front part (less tense or easily deformable under internal pressure) was proposed to explain the migration of *Amoeba proteus* [20] but also plant pollen tubes [21] and multicellular *Dictyostelium* slugs [11]. In all these examples, the source of asymmetry is structural and stable in the sense that it can be captured by an appropriate microscopy technique. Another model of locomotion by peristalsis assumes that the source of symmetry breaking is purely dynamics. It was proposed to describe the motion of some animals (worms, snails, etc.). In this model, two waves are propagating along the organism axis with the same speed and the same direction, a wave of local deformation (or local cell contraction) and a wave of local adhesion (or local friction) with the substrate. If there is a phase lag between them, the deformation is translated into directional motion [22]. Waves of deformations were already observed in small tadpole-like

microplasmodia by some of us [16], and it was recently observed that travelling waves of contractile traction stresses also propagate [23].

In this work, we did not find such tadpole-like shapes and we did not focus on that issue. However, we could record a few experiments showing microplasmodia that suddenly start to move from an albeit pulsating but immobile state (see last frames of electronic supplementary material, movie M3; figures 3*h*, 5*b* and 7). Cell shape as well as traction forces or fibril distribution experience drastic changes when the cell starts to move in a given direction but it is difficult to find any simple phase rule. For instance in figure 7, when two different parts are periodically contracting in phase, these two parts compete to push each other and little net migration is observed. But once the two parts start to contract in counter-phase, these two parts come to take different roles, a pushing and a pushed part and finally a pushed part expands and becomes a migration front of plasmodium. On the opposite, in figure 3*h* (electronic supplementary material, movie M4), the two parts of the dumbell-shaped microplasmodium are mostly contracting in counter-phase (figure 4*f*), but we do not observe initially any net displacement of the centre of mass. It is hence possible that the true event triggering the net locomotion comes from a structural asymmetry (e.g. softening of the front actomyosin cortex, sudden increase in the local pressure due to changes in the invagination and fibrillar networks). To clarify this, we need more precise and multiple measurements that enable one to see time difference between force generation, fibril formation (not only thick fibrils but also thinner ones), protoplasmic streaming and net displacement of the microplasmodium. It may be a challenge in future studies.

5. Conclusion

This study strongly reinforces the idea that a common mechanism controls the amoeboid migration of various species with various sizes. When viewed at sufficiently high temporal resolution, cyclic periodicities are found in the cellular shape changes of many crawling cell types, including neutrophils [24], *Dictyostelium discoideum*, *Physarum* and *Amoeba proteus* [25]. An asymmetry in the forces along anterior–posterior axis seems a prerequisite to initiate cell motion. The novelty of this study arises from the complex structure of the microplasmodia that generate new types of traction force maps. In particular, the annular contractile units under the heads of chain type microplasmodia actively regulated by the fibrillar contractile activity were never reported. Although very complex, a remarkable periodic oscillation in force transmission to the substratum with a period of 1–2 min was always identified. Such oscillations were also reported for *Dictyostelium* single cells [12] but with not such a regularity and clarity probably due to the smaller system size that makes more difficult the initiation of self-sustained behaviours. *Physarum* appears hence still as a valuable system to study the very basic mechanisms of cell migration.

Acknowledgements. We thank Y. Hayakawa, M. Sano and H. Tanimoto for fruitful discussions.

Funding statement. J.-P.R. acknowledges support from the Japan Society for the Promotion of Science (Invitation Fellowship for Research in Japan, Long Term, FY2010), from ElyTLab (Lyon-Tohoku) International Laboratory and from the Center for Interdisciplinary Research (CIR, Tohoku University). The authors acknowledge the Institute of Multiscale Science and Technology (iMUST) supported by the French ANR. This research was partially supported by JSPS KAKENHI grant no. 26310202, and by a Grant-in-Aid for Scientific Research on Innovative Areas 'Fluctuation and Structure' (no. 25103006) and 'Cross talk between moving cells and microenvironment' (no. 25111726) from Mext Japan.

References

1. Kessler D. 1982 Plasmodial structure and motility. In *Cell biology of physarum and didymium: organisms, nucleus, and cell cycle,* vol. 1 (ed. H Aldrich), pp. 145–208. New York, NY: Academic Press.
2. Wohlfarth-Bottermann KE, Fleischer M. 1976 Cyclic aggregation patterns of cytoplasmic F-actin coordinated with oscillating tension force generation. *Cell Tissue Res.* **165**, 327–344. (doi:10.1007/BF00222437)
3. Nagai R, Yoshimoto Y, Kamiya N. 1978 Cyclic production of tension force in the plasmodial strand of *Physarum polycephalum* and its relation to microfilament morphology. *J. Cell Sci.* **33**, 205–225.
4. Ishigami M, Kuroda K, Hatano S. 1987 Dynamic aspects of the contractile system in Physarum plasmodium. III. Cyclic contraction–relaxation of the plasmodial fragment in accordance with the generation–degeneration of cytoplasmic actomyosin fibrils. *J. Cell Biol.* **105**, 381–386. (doi:10.1083/jcb.105.1.381)
5. Yoshiyama S, Ishigami M, Nakamura A, Kohama K. 2010 Calcium wave for cytoplasmic streaming of *Physarum polycephalum*. *Cell Biol. Int.* **34**, 35–40.
6. Alim K, Amselem G, Peaudecerf F, Brenner MP, Pringle A. 2013 Random network peristalsis in *Physarum polycephalum* organizes fluid flows across an individual. *Proc. Natl Acad. Sci. USA* **110**, 13 306–13 311. (doi:10.1073/pnas.1305049110)
7. Kamiya N. 1981 Physical and chemical basis of cytoplasmic streaming. *Annu. Rev. Plant Physiol.* **32**, 205–236. (doi:10.1146/annurev.pp.32.060181.001225)
8. Gawlitta W, Wolf KV, Hoffmann H-U, Stockem W. 1980 Studies on microplasmodia of *Physarum polycephalum*. I. Classification and locomotion behavior. *Cell Tissue Res.* **209**, 71–86. (doi:10.1007/BF00219924)
9. Bray D. 2001 *Cell movements: from molecules to motility*. New York, NY: Garland Publishing.
10. Rieu JP, Saito T, Delanoë-Ayari H, Sawada Y, Kay R. 2009 Migration of *Dictyostelium* slugs: anterior-like cells may provide the motive force for the prespore zone. *Cell Motil. Cytoskeleton* **66** 1073–1086. (doi:10.1002/cm.20411)
11. Rieu JP, Delanoë-Ayari H. 2012 Shell tension forces propel *Dictyostelium* slugs forward. *Phys. Biol.* **9**, 066001. (doi:10.1088/1478-3975/9/6/066001)
12. Delanoë-Ayari H, Iwaya S, Maeda YT, Inose J, Rivière C, Sano M, Rieu JP. 2008 Changes in the magnitude and distribution of forces at different *Dictyostelium* developmental stages. *Cell Motil. Cytoskeleton* **65**, 314–331. (doi:10.1002/cm.20262)
13. Oldenbourg R. 1996 A new view on polarization microscopy. *Nature* **381**, 811–812. (doi:10.1038/381811a0)
14. Ishigami M. 1986 Dynamic aspects of the contractile system in *Physarum* plasmodium. I. Changes in spatial organization of the cytoplasmic fibrils according to the contraction–relaxation cycle. *Cell Motil. Cytoskeleton* **6**, 439–447. (doi:10.1002/cm.970060502)
15. Achenbach F, Naib-Majani W, Wohlfarth-Bottermann KE. 1979 Plasmalemma invaginations of Physarum dependent on the nutritional content of the plasmodial environment. *J. Cell Sci.* **36**, 355–359.
16. Matsumoto K, Takagi S, Nakagaki T. 2008 Locomotive mechanism of physarum plasmodia based on spatiotemporal analysis of protoplasmic streaming. *Biophys. J.* **94**, 2492–2504. (doi:10.1529/biophysj.107.113050)
17. Wohlfarth-Bottermann KE. 1974 Plasmalemma invaginations as characteristic constituents of plasmodia of *Physarum polycephalum*. *J. Cell Sci.* **16**, 23–37.
18. Delanoë-Ayari H, Rieu JP, Sano M. 2010 4D traction force microscopy reveals asymmetric cortical forces in migrating *Dictyostelium* cells. *Phys. Rev.*

Lett. **105**, 248103. (doi:10.1103/PhysRevLett.105.248103)

19. Renkawitz J, Sixt M. 2010 Mechanisms of force generation and force transmission during interstitial leukocyte migration. *EMBO Rep.* **11**, 744–750. (doi:10.1038/embor.2010.147)
20. Stockem W, Hoffmann H-U, Gawlitta W. 1982 Spatial organization and fine structure of the cortical filament layer in normal locomoting *Amoeba proteus*. *Cell Tissue Res.* **221**, 505–519. (doi:10.1007/BF00215699)
21. Fayant P, Girlanda O, Chebli Y, Aubin CE, Villemure I, Geitmann A. 2010 Finite element model of polar growth in pollen tubes. *Plant Cell* **22**, 2579–2593. (doi:10.1105/tpc.110.075754)
22. Tanaka Y, Ito K, Nakagaki T, Kobayashi R. 2011 Mechanics of peristaltic locomotion and role of anchoring. *J. R. Soc. Interface* **9**, 222–233. (doi:10.1098/rsif.2011.0339)
23. Lewis OL, Zhang S, Guy RD, del Alamo JC. Submitted. Coordination of contractility, adhesion and flow in migrating Physarum amoebae.
24. Ehrengruber MU, Deranleau DA, Coates TD. 1996 Shape oscillations of human neutrophil leukocytes: characterization and relationship to cell motility. *J. Exp. Biol.* **199**, 741–747.
25. Satoh H, Ueda T, Kobatake Y. 1985 Oscillations in cell shape and size during locomotion and in contractile activities of *Physarum polycephalum*, *Dictyostelium discoideum*, *Amoeba proteus* and macrophages. *Exp. Cell Res.* **156**, 79–90. (doi:10.1016/0014-4827(85)90263-0)